

# Wind assessment in complex terrain with the numeric model Aiolos – implementation of the influence of roughness changes and stability

Ulrich Focken, Detlef Heinemann, Hans-Peter Waldl  
 Department of Energy and Semiconductor Research, Faculty of Physics,  
 Carl von Ossietzky University of Oldenburg, D-26111 Oldenburg, German  
 FAX ++49 441 798-3326, e-mail: office@ehf.uni-oldenburg.de

The method of the European Windatlas (EWA) gives good results for the wind potential estimation in flat areas. But besides many investigations, there is no reliable standard algorithm for wind potential estimation in complex terrain. Within the framework of a masterthesis the initialisation of the mass consistent model Aiolos is modified with regard to the influence of roughness changes and the thermal stratification. Wind potential assessments of two sites in the low mountain range "Erzgebirge" in Germany are compared with measured data.

Keywords: Boundary Layer, Micrositing, Windpotential, Complex Terrain

## 1 Introduction

It's general practice to use mass consistent models for simulation of stationary three dimensional wind fields in complex terrain. The advantage of a mass consistent model compared with primitive equation models is relatively short computing time. Therefore it is not possible to look at complex phenomena as turbulence or heat flux.

The initialisation of Aiolos, which is developed from the well known model NOABL, is changed within this framework. The influence of roughness changes on the terrain surface and thermal stratification of the atmosphere are taken into account. Due to good results of the EWA in flat terrain it serves the basis for this model.

## 2 Initialisation

To simulate the air-flow, the boundary layer is divided into a grid of  $x \times y \times z$  boxes. with equidistant horizontal box distances. The vertical coordinate is transformed in a terrain following  $\sigma$ -coordinate. The space between these  $\sigma$ -levels decreases to get a higher resolution near the surface. For each box a "first guess" of the wind velocity vector has to be determined. This step is the most important for a mass consistent model, because the correction of this initialisation wind field uses only the equation of mass conservation.

Thus the initialisation wind field has a big influence on the results opposed to the primitive equation models.

### 2.1 Initialisation of Aiolos

The geostrophic wind is the basis to calculate the initialisation wind field. The simplified geostrophic drag law

$$u_* = \frac{0.5 G}{\ln \frac{G}{f z_0}}$$

connects the geostrophic wind and the surface layer. The vertical wind profile for each grid point is calcu-

lated by the logarithmic windprofil for neutral conditions, which is fitted to the geostrophic wind by a polynomial of third order

$$v = \frac{u_*}{k} \ln \left( \frac{z}{z_0} \right) + 3 \cdot \left( \frac{z}{z_G} \right)^2 - 2 \cdot \left( \frac{z}{z_G} \right)^3$$

where  $z_G$  is the height of the geostrophic wind. Calculations for flat terrain showed unsatisfactory correspondence with measurements. That is why the models of the EWA are used for the initialisation.

### 2.2 The new initialisation

For the calculation of wind potential in flat areas the EWA method uses 3 different models:

- the shelter model
- the roughness model
- the stability model

The shelter model is omitted here.

#### *The stability model*

For the calculation of original Aiolos a neutral thermal stratification situation is assumed. But for a north european situation a light stable boundary layer is found in the yearly average. For that reason the logarithmic windprofile is modified by the stability function  $\psi$ :

$$v = \frac{u_*}{k} \ln \left( \frac{z}{z_0} - \psi \left( \frac{z}{L} \right) \right)$$

$L$  is the Monin-Obukov-Length. The stability function

$$\psi(z/L) = \begin{cases} \left(1 - 16 \frac{z}{L}\right)^{\frac{1}{4}} - 1 & \text{for unstable stratification} \\ (-4.7 \frac{z}{L}) & \text{for stable stratification} \end{cases}$$

is taken from [Jens84].

### The roughness model

The calculation of a wind profile in Aiolos uses only the roughness of this grid point, not the surroundings. Consequently upstream roughness has no influence on the wind profile.

Figure 1 shows a typical situation with two roughness

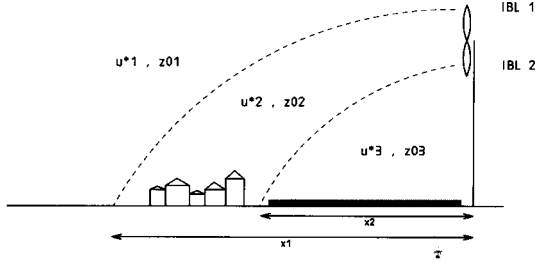


Figure 1: Evolution of an internal boundary layer at a roughness change. The friction velocity  $u^*$  and the roughness length  $z_0$  are the characteristic sizes within a layer.

changes. For wind blowing from the left there develops two internal boundary layers (IBL), so at the site of the turbine the profile is divided into three sections. The roughness of the water on the left in Figure 1 determines the top section of the wind profile. Between the layers, at hub height of the wind turbine, the wind velocity is determined by the roughness of the town. Only in the bottom section the local roughness of the site is important. An expression for the height of the IBL is given by [pano73]:

$$\frac{h}{z_{0max}} \left( \ln \left( \frac{h}{z_{0max}} \right) - 1 \right) = 0.9 \frac{x_n}{z_0}$$

with

$$z_{0max} = \max(z_{01}, z_{02})$$

where  $x_n$  defines the distance from the site (see Figure 1). Sempreviva [semp86] shows that this equation is only valid for near roughness changes and introduced two additional layers at 9% and 30% height of the IBL.

So the wind profile for two roughness changes is:

$$u(z) = \begin{cases} \frac{u_1^*}{\kappa} \ln \left( \frac{z}{z_{01}} \right) & \text{for } 0.3 \cdot h_1 \leq z \\ u'' + (u''' - u'') \frac{\ln \left( \frac{z}{0.3 \cdot h_2} \right)}{\ln \left( \frac{0.3 \cdot h_1}{0.3 \cdot h_2} \right)} & \text{for } 0.3 \cdot h_2 \leq z < 0.3 \cdot h_1 \\ u' + (u'' - u') \frac{\ln \left( \frac{z}{0.09 \cdot h_2} \right)}{\ln \left( \frac{0.3 \cdot h_2}{0.09 \cdot h_2} \right)} & \text{for } 0.09 \cdot h_2 \leq z < 0.3 \cdot h_2 \\ \frac{u_3^*}{\kappa} \ln \left( \frac{z}{z_{03}} \right) & \text{for } z < 0.09 \cdot h_2 \end{cases}$$

with

$$u' = \frac{u_3^*}{\kappa} \ln \left( \frac{0.09 \cdot h_2}{z_{03}} \right)$$

$$u'' = \frac{u_2^*}{\kappa} \ln \left( \frac{0.3 \cdot h_2}{z_{02}} \right)$$

$$u''' = \frac{u_1^*}{\kappa} \ln \left( \frac{0.3 \cdot h_1}{z_{01}} \right)$$

where  $u^*$  is the friction velocity and  $\kappa$  the von-Kármán constant.

To apply this model the surroundings of a site are divided into 12 wind directions of 30 degrees. The roughness changes has to be determined for each wind direction. The difference to the application WASP are 10000 points instead of one and it is not possible to determine the roughness changes from a topographical map. Therefore we developed an algorithm to calculate a grid of roughness changes for 12 sectors from a grid of roughness lengths.

The first step of this algorithm is to average the roughness length in a tangential stripe with the width of a box. After that stripes with similar roughness are averaged.

### 2.3 The numerical procedure of Aiolos

To start out with the initialisation wind field  $\vec{v}_0$  the correction wind  $\vec{v}_k$  field is calculated, which defines the correction to minimize the local divergence.

$$\begin{aligned} u &= u_0 + u_k \\ v &= v_0 + v_k \\ w &= w_0 + w_k \end{aligned}$$

By adding the correction wind field the vorticity is assumed to be constant, so

$$\nabla \times \vec{v}_k = 0.$$

Consequently the correction wind field can be calculated out of a perturbation velocity potential  $\Phi$

$$u_k = \tau_h \frac{\partial \Phi}{\partial x}, \quad v_k = \tau_h \frac{\partial \Phi}{\partial y}, \quad w_k = \tau_v \frac{\partial \Phi}{\partial z}.$$

The horizontal and vertical transmission coefficients  $\tau_h$  and  $\tau_v$  are an easy way to simulate the thermal stratification during the simulation.

For a constant density the equation of mass conservation becomes

$$\frac{\partial u}{\partial x} + \frac{\partial v}{\partial y} + \frac{\partial w}{\partial z} = 0$$

By substituting preliminary equations in the last one a poisson equation is obtained

$$\frac{\partial}{\partial x} \left( \tau_h \frac{\partial \Phi}{\partial x} \right) + \frac{\partial}{\partial y} \left( \tau_h \frac{\partial \Phi}{\partial y} \right) + \frac{\partial}{\partial z} \left( \tau_v \frac{\partial \Phi}{\partial z} \right) = - \left( \frac{\partial u_0}{\partial x} + \frac{\partial v_0}{\partial y} + \frac{\partial w_0}{\partial z} \right).$$

which must be solved. For this a Successive-Overrelaxation-Procedure is used [rich96], [tracy78], [steff91].

### 3 Results

For two sites in low mountain range in Germany, the "Erzgebirge", wind potential estimations are compared with measured data.

Figure 2 shows the roughness of the calculation area of Ragewitz by using the roughness length, which varies from  $z_0 = 0.05$  meters for farmland to  $z_0 = 0.6$  meters for a city in the east. There are also two small areas of forest in the south and northeast.

Figure 3 shows the calculated wind field for a geostrophic wind of 15 m/s from the northwest at 36 m height. The difference between original and new initialisation is the decreased windspeed in the wake of high roughnesses as can be seen by the town in the east. This effect can also be observed for small villages in the northwest.

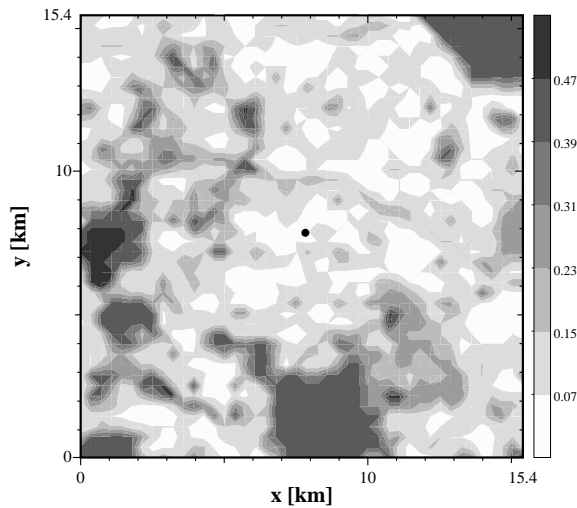


Figure 2: Map of roughness length  $z_0$  [m] for the area of Ragewitz.

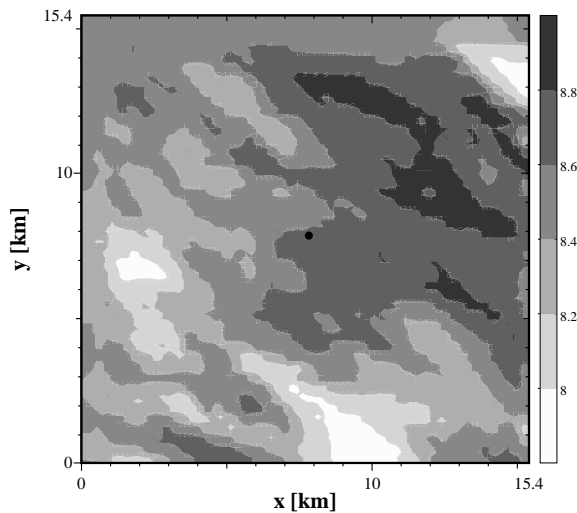


Figure 3: Horizontal wind field in a height of 36 m. Geostrophic wind from the northwest.

The corresponding orography is shown in Figure 4. The surface altitude varies from 120 m in a river

valley up to 240 m at the top of a hill. The yearly mean windspeed is calculated from 480 situations (40 windspeeds and 12 sectors) weighted by the frequency of occurrence of the geostrophic wind. The result is shown in Figure 5. It can be seen that the windspeed increases for higher areas. The second important parameter for high windspeeds is the height gradient as can be seen at higher windspeeds at the two foothills northwest the mainhill.

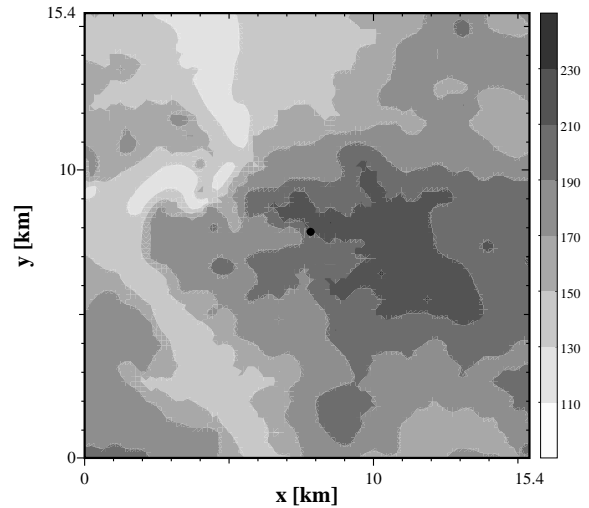


Figure 4: Orographical structure (altitude [m]) of Ragewitz.

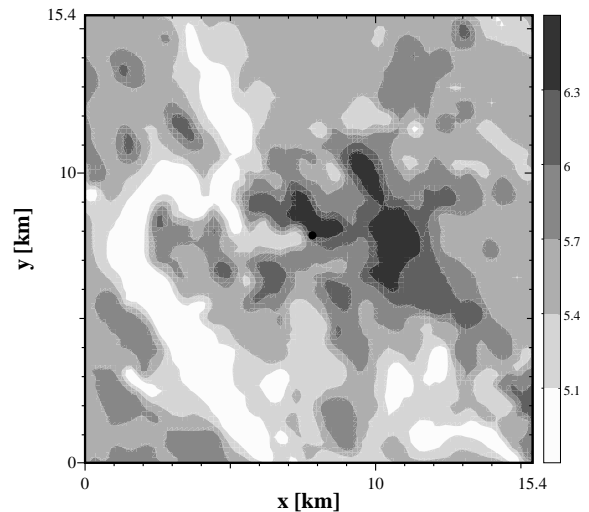


Figure 5: Field of yearly mean windspeed of Ragewitz in an height of 36 m with influence of roughness changes and stability.

Until 1992 a measurement tower is placed in the middle of the area. Simulations with new and old initialisations are compared with this measurement data. In the following "new windspeed" refers to the results including the roughness model, and "old windspeed" refers to the original initialisation.

Table 1 shows the difference between simulated and measured windspeed. The deviation for the new

	k	v [m/s]	P [W/m <sup>2</sup> ]
old initialisation	1.77	5.59	234
new initialisation	1.84	6.34	322
measurement data	2.08	6.41	295

Table 1: Results from Ragewitz

initialisation is only 1.1 % compared with 12.8 % deviation for the old initialisation. The mean power density depends not only on the windspeed but also on the k-factor of the weibull distribution. Therefore the deviation of the mean power density is higher than expected. In this case also the estimation with the new initialisation is much better.

	k	v [m/s]	P [W/m <sup>2</sup> ]
old initialisation	1.79	5.40	207
new initialisation	1.84	6.16	297
measurement data	2.01	6.96	374

Table 2: Results from Hermsdorf

The second site Hermsdorf is situated from 550 m up to 800 m and is determined by height gradients up to 20 %. As expected, the differences between the measurements and the simulations are higher. The underestimation of the k-factor of the weibull distribution is the same as in Ragewitz. Also calculations with the EWA show the same behaviour. This results out of a wrong mapping of geostrophic wind to the surface wind through the geostrophic drag law.

#### 4 Conclusion

The application of a mass-consistent model like Aiolos is restricted to simulation of orographical effects. The initialisation wind field has a big influence on the result and should describe the flow situation without orography quite well. Because that is not the case for the original initialisation the models of the EWA are used for calculate the initialisation wind field.

For two sites in the low mountain range in Germany the difference between measurement and estimated mean windspeed and mean power density decreases. However the predicted power density is compared with the wind speed respectively too high. This is caused by a wrong estimation of the wind speed distribution which results out of a false mapping of the geostrophic wind to the surface wind through the geostrophic drag law.

Of course two simulations are a small basis, so further comparisons to measured data are necessary to validate this model.

#### References

- [fock98] Ulrich Focken. *Windpotentialbestimmung in komplexem Gelände mit dem numerischen Strömungsmodell Aiolos – Optimierung des Verfahrens in bezug auf Rauheits- und Stabilitätseinflüsse*. Diplomarbeit Carl-von-Ossietzky Universität Oldenburg 1998
- [rich96] Richard Müller. *Untersuchung zur Windpotentialbestimmung in gegliedertem Gelände*. Diplomarbeit Carl-von-Ossietzky Universität Oldenburg 1996
- [steff91] F. Steffany. *Anwendung eines massenkonsistenten Strömungsmodells im 'Microscale'*. Diplomarbeit Universität Köln 1991
- [jens84] N. O. Jensen, E.L. Petersen, I. Troen. *Extrapolation of mean wind statistics with regard to wind energie applications*. World Meteorological Organisation WCP-86.85 1984
- [lala85] D.P.Lalas. *Wind Energy Estimation and Siting in Complex Terrain*. International Journal of Solar Energy 1985. Vol.3
- [ewa90] I. Troen, E.L. Petersen. *Europäischer Windatlas*. Risø National Laboratory Roskilde Denmark 1990
- [trifo90] D. Trifonopoulos, G. Bergeles. *Wind Energy Potential over the Evia Wind Park - Greece*. EWEC Madrid 1990
- [semp86] A.M Semprevia, I. Troen, A. Lavagnini. *Modelling of Wind Power Potential over Sardinia*. EWEC Rom 1986
- [pano73] H. A. Panofsky. *Tower Climatology*. Workshops on Micrometeorology, American Meteorological Society, 1973
- [tracy78] R. M. Tracy, G. T. Phillips, P. C. Patnaik. *Developing a Site Selection Methodology for Wind Energie Conversion Systems*. DOE/ET/20280-3 NTIS 1978